# SPOKE CAVITIES: AN ASSET FOR THE HIGH RELIABILITY OF A SUPERCONDUCTING ACCELERATOR

## *STUDIES AND TESTS RESULTS OF A $\beta$ = 0.35, TWO-GAP PROTOTYPE AND ITS POWER COUPLER AT IPN ORSAY*

**C. Miélot**
Institut de Physique Nucléaire
Orsay, France

**Abstract**

Taking into account the PDS-XADS requirements concerning accelerating field, quality factor and reliability, two spoke-type cavities have been designed at IPN Orsay. One of them has been successfully tested and the second one is currently being fabricated. This paper reports on the excellent performance of the first cavity, substantially exceeding the requirements, which make spoke cavities an attractive solution for a reliable PDS-XADS proton driver.

## Introduction

Studies on spoke cavities are in progress at IPN Orsay. Taking into account the requirements defined by deliverable D57 of PDS-XADS [1,2], a b = 0.35 spoke cavity has been designed. Fabricated by CERCA, the cavity was tested at IPN. A second spoke cavity with b = 0.15 has been designed and is presently being fabricated. As shown in P. Pierini's contribution to this conference, superconducting spoke cavities seem to be an attractive solution for the low b section of the XADS accelerator. In this paper, subsequent to a short description of the design and fabrication process, we will discuss the results of the tests performed at IPN and demonstrate their good performances with respect to the established requirements. One of the main imperatives for the whole accelerator is reliability, such that the feasibility of producing this system on industrial scale can be shown. The system must be fault tolerant, and the number of beam trips should be less than five per year. The result of the tests will show that using spoke cavities for the low b section is a good strategy for achieving the goal of reliability.

## Design and fabrication

These cavities are referred to as "spoke" cavities within the accelerators community because of the "spoke-like" part that goes through the outer wall of the cavity (see Figure 1). This spoke defines two gaps in which the electric field can accelerate the proton beam that goes through the central hole of the spoke. The accelerating field of these resonating cavities is driven by an external RF transmitter linked to the cavity by a coupling port. The cavities are made of bulk niobium (superconducting metal at working temperature 4 K). The b = 0.35 cavity, named "AMANDA", had been designed with the help of the electromagnetic code MAFIA. The optimisation of $E_{pk}/E_{acc}$ (the ratio of peak electric field on the wall of the cavity and accelerating field) and of $B_{pk}/E_{acc}$ (magnetic peak field out of accelerating field) lead to a diameter $D$ of one-third of the accelerating length: $D = 1/3\ L_{acc}$. The shape of the central spoke has been designed to reduce $B_{pk}/E_{acc}$ (optimisation of the spoke extremities diameter) and to increase the transit time factor $T_t$, given by D$E = e.V.T_t$, where D$E$ is the energy gain, $e$ the proton charge and $V$ the maximum voltage in the gap (see Figure 1). To ensure rigidity and good mechanical performances, stiffeners have been added on the flanges of the cavity as shown in Figure 2.

Fabrication was ensured by CERCA, using specially designed tools. The centre shape of the spoke was made possible by squeezing the cylinder while the rest of the spoke was strictly maintained. Table 1 shows the main characteristics (in mm) of the b = 0.35 spoke cavities.

**Figure 1. Shape of a spoke cavity (CATIA software)**

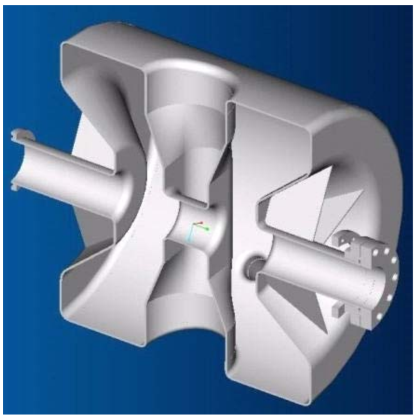

**Figure 2. Stiffeners on the cavity flanges (ACORD-CP software)**

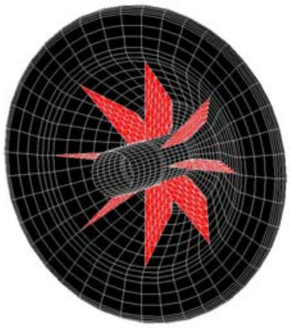

**Table 1. Main characteristics of AMANDA (in mm)**

| | |
|---|---|
| Cavity diameter | 408 |
| Total length | 354 |
| Spoke base diameter | 118 |
| Spoke centre thickness | 67 |
| Spoke centre width | 147 |
| Gap centre to gap centre | 150 |
| Iris to iris | 200 |
| Beam tube length | 150 |
| Beam tube aperture | 60 |

## Tests results

### *Lorentz force coefficient*

Measuring the frequency shift with the variation of $E_{acc}$, we could deduce the value of the Lorentz force coefficient, which is K = -5.6 Hz/(MV/m)$^2$, shown in Figure 3. The measures have been taken with a stiffening system mounted on the cavity. This value is in good agreement with the predicted value of -8 Hz/(MV/m)$^2$, given the numerous approximations in the code, meaning that the mechanical behaviour of the cavity is better than the more challenging behaviour of low-b elliptical cavities.

**Figure 3. Frequency (MHz) vs. $E_{acc}^2$ (MV/m)$^2$**

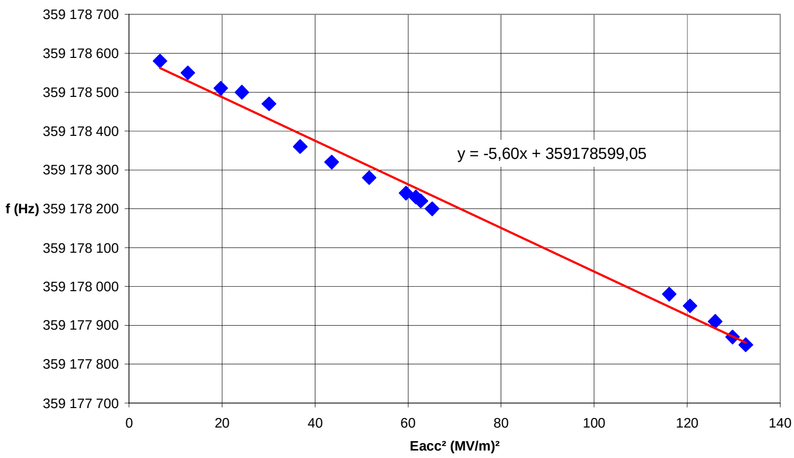

### *Surface resistance*

The first measure of surface resistance [Figure 4, measuring $G/Q_0$ (diamonds) where $G$ is the given geometrical factor of the cavity, $G = R_s.Q_0$, with the surface resistance $R_s$ and $Q_0$ the quality factor] gave a value of 10 nW for residual resistance. After staying 67 hours at 100 K another measure gave 70 nW for residual resistance (squares, Figure 4). The value of residual resistance was found by comparison with empirical formula for surface resistance:

$$R_s = 9.10^{-5}.\frac{1}{T}.f^2.\exp\left(-1.83.\frac{T_c}{T}\right) + R_{res}$$

where $T$ is the temperature, $f$ the frequency and $T_c$ is the critical temperature of niobium ($T_c$ = 9.2 K). This value is appropriated under the condition that the cavity is protected from the 100 K effect; this is an important point that will have to be taken into account for minimising the losses on the cavity walls. Indeed, when left at a temperature around 100 K, the hydrogen that is inside the niobium precipitates into components which in term increase $R_s$.

**Figure 4. Surface resistance of the cavity walls (W) vs. 1/Pcav (1/W)**

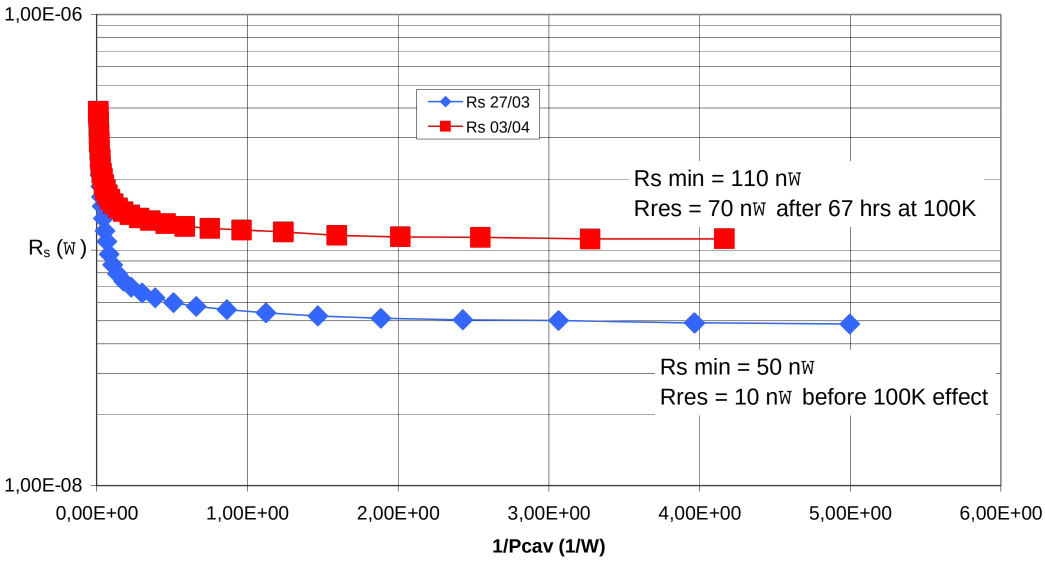


### *The quality factor $Q_0$*

Measures of $Q_0$ vs. $E_{acc}$ were performed under various conditions: with and without high pressure rinsing (HPR), with ultra-pure water, with different coupling positions, and with and without helium processing. The main results are given in Figures 5 and 6.

After 67 hours at 100 K the maximum $E_{acc}$ is down to 11.9 MV/m with $Q_0 = 3.10^8$ (see Figure 5). These tests were performed using the beam tube as coupling port. Then it can be noted that HPR is absolutely necessary; as show in Figure 6, this usual processing allows reaching high $E_{acc}$. The limitation encountered during the first test (without HPR, diamonds in Figure 6) was due to multi-pacting. Multi-pacting is a field-limiting resonant phenomenon due to secondary emitted electrons. Even after HPR – but without He processing – the same multi-pacting barrier was encountered between 1.5 MV/m and 2 MV/m. He processing is another usual process, used in cavity preparation and tests. It consists

**Figure 5. $Q_0$ vs. $E_{acc}$ (MV/m)**

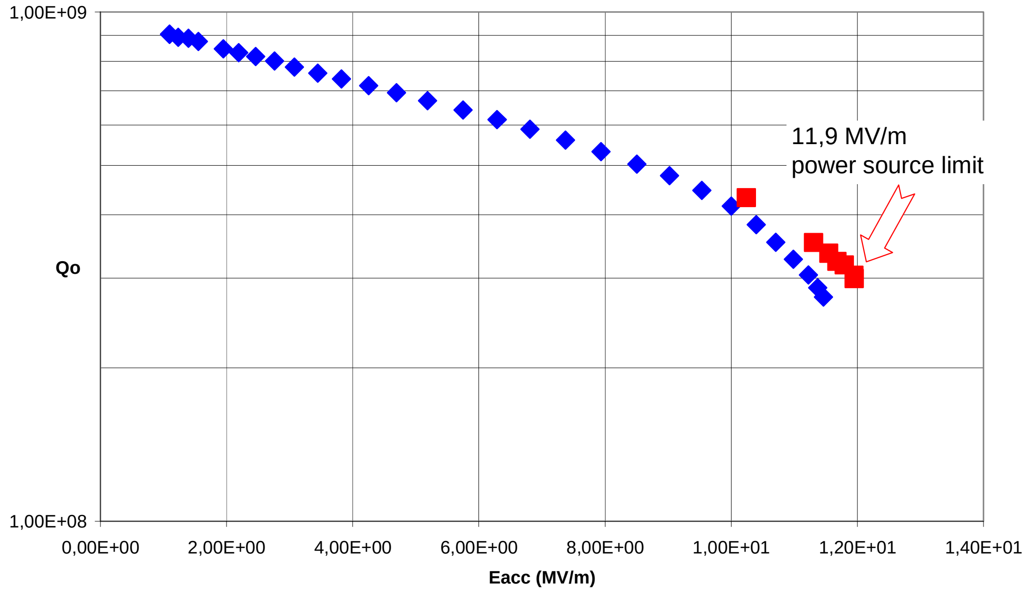


**Figure 6. $Q_0$ vs. $E_{acc}$ without HPR (diamonds), with HPR and without He processing (squares) and with both HPR and He processing (triangles)**

*The red star indicates the requirements for PDS-XADS: $E_{acc}$ = 7 MV/m with $Q_0 = 5.10^8$.*

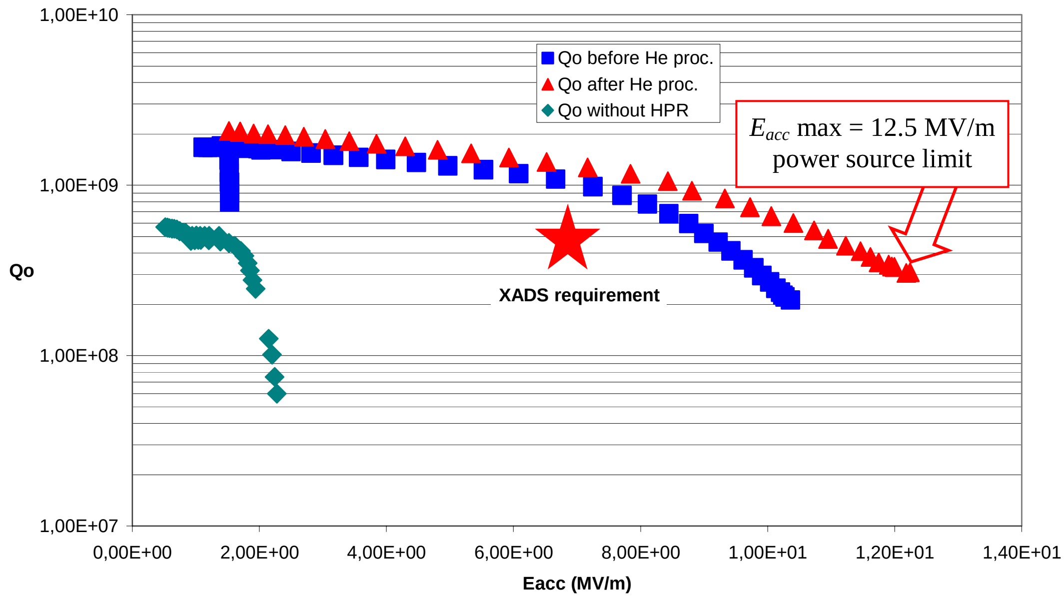


of introducing a low pressure of He ($10^{-5}$ mbars) inside the cavity, and using RF power to produce arcing that destroys electron emitting sites. After two He processings we could achieve $E_{acc}$ = 12.55 MV/m ($Q_0 = 3.10^8$); this maximum is due to source limitation (no quench). Within that test we could also achieve $Q_0 = 2.10^9$ at low field. Regarding the requirements for PDS-XADS, it can be seen that we have achieved a comfortable performance margin that is a very positive point for reliability. Table 2 sums up the results of the tests.

**Table 2. Main characteristics of the tests results**

| Test no. | Rinsing | Coupling | Low field $Q_0$ | $E_{acc}$ max |
|---|---|---|---|---|
| 1<br>January 2003 | No HPR | Coupling port | 5.00E+08 | 2.3 MV/m |
| 2<br>March 2003 | HPR | Beam tube | 2.10E+09 | 12.2 MV/m |
| 3<br>July 2003 | HPR | Coupling port | 4.00E+08 | 12.55 MV/m |

### *Losses on antenna, coupling port position*

During the last test we used a variable coupler to feed the RF power through the coupling port. Figure 7 shows the increase of the losses on the antenna when it was moved from a 23-mm position to 11 mm within the port. This meant that the coupling port was set in an area where the magnetic field was rather high, so it was decided to proceed with numerical calculations to choose an optimised location for the coupling port. The calculations were also performed to determine an accurate port diameter in order to avoid multi-pacting problems. The results of the simulations are given in the next section.

**Figure 7. $Q_0$ vs. position of the antenna inside the coupling port (mm)**

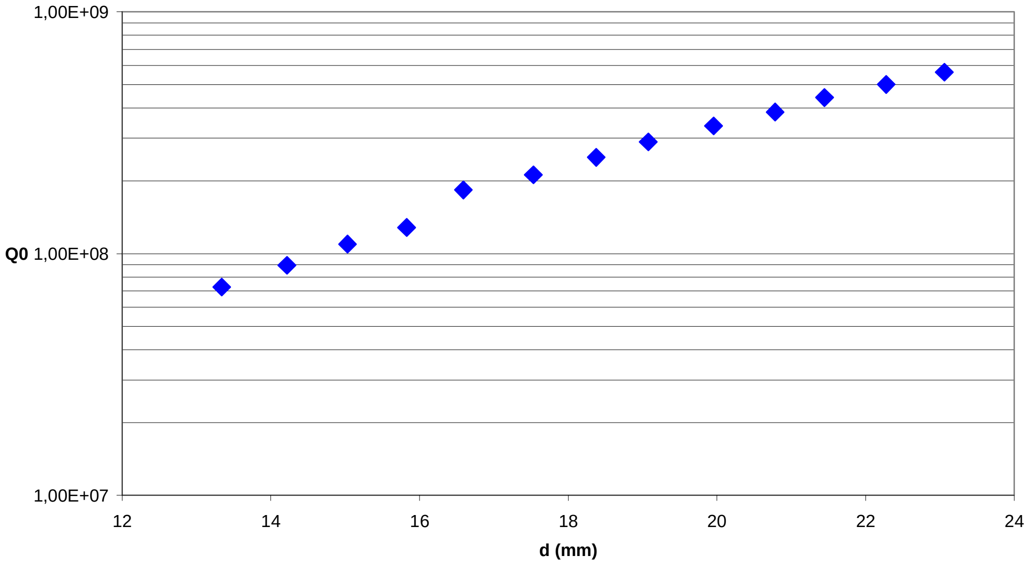


## Numerical simulations

### *Position and diameter of the coupling port*

All the numerical simulations are undertaken using the ANSOFT HFSS electromagnetic code. Regarding multi-pacting occurrences and compromising with mechanical limitations, we chose a port diameter F = 53 mm. Table 3 shows the RF threshold power multi-pacting barrier (in kW) for different port diameters and for orders 1 to 10. The lower the order, the more often this multi-pacting barrier can occur. Since 20 kW must be fed to the cavity, the diameter chosen must allow to sustain such a power without a multi-pacting barrier. It is reasonable to avoid multi-pacting until order 3 regarding the low probability of a higher order barrier to occur. In Table 3, the threshold powers that can be overcome with no multi-pacting regarding the 20 kW power to be carried through the line are shaded in grey. This means, for example, that with the choice of $F_{port}$ = 50 mm, an order 2 multi-pacting barrier occurs at $P$ = 16.38 kW. As the power in the line is 20 kW, this multi-pacting order is reached. As this order is low enough to be dangerous, we want to avoid it. With a $F_{port}$ = 56 mm, this order requires 25.77 kW to start, thus limiting the power to 20 kW will eliminate such a possiblity.

**Table 3. Multi-pacting barriers for order 1 to 10 for different port diameters. The diameter of the antenna is given for line impedance of 50 W.**

| Multi-pacting order | $F_{port}$ (mm) | 30 | 50 | 56 | 60 | 70 | 100 |
|---|---|---|---|---|---|---|---|
| | $F_{ant}$ (mm) | 13.03 | 21.72 | 24.32 | 26.06 | 30.4 | 43.43 |
| 1 | | 3.07 | 23.7 | 37.3 | 49.15 | 91.06 | 379.26 |
| 2 | | 2.12 | 16.38 | 25.77 | 33.96 | 62.92 | 262.05 |
| 3 | | 1.2 | 9.41 | 14.81 | 19.52 | 36.16 | 150.61 |
| 4 | | 0.72 | 5.56 | 8.76 | 11.54 | 21.38 | 89.04 |
| 5 | | 0.45 | 3.46 | 5.44 | 7.17 | 13.28 | 55.33 |
| 6 | | 1.29 | 2.28 | 3.59 | 4.73 | 8.76 | 36.47 |
| 7 | | 0.21 | 1.61 | 2.53 | 3.34 | 6.19 | 25.79 |
| 8 | | 0.16 | 1.24 | 1.95 | 2.57 | 4.76 | 19.82 |
| 9 | | 0.13 | 1.04 | 1.63 | 2.15 | 3.99 | 16.63 |
| 10 | | 0.12 | 0.95 | 1.49 | 1.96 | 3.64 | 15.16 |

Once the diameter was determined, the numerical simulation concerning the port position was undertaken. The position is given by the angle of the port with the spoke. The initial position is given by q = 45° in Figure 8.

**Figure 8. Start situation: port angle = 45**

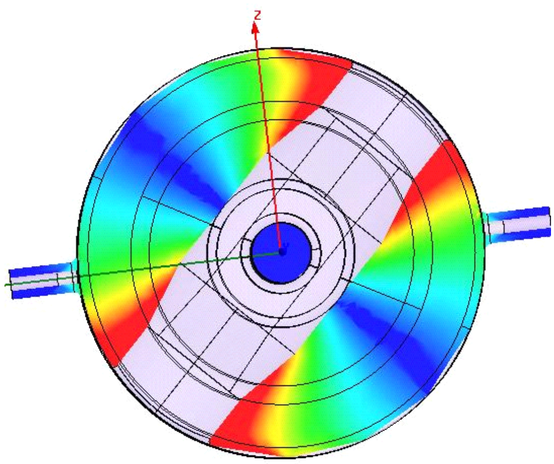


The normalised losses decrease a q increase from 45° to 90°. Figure 10 shows the integrated squared magnetic field on the antenna surface that is actually in contact with the field for the AMANDA cavity. It was therefore decided that the next cavity would be fabricated with a 90° angle, as shown in Figure 9.

**Figure 9. Final situation: port angle = 90**

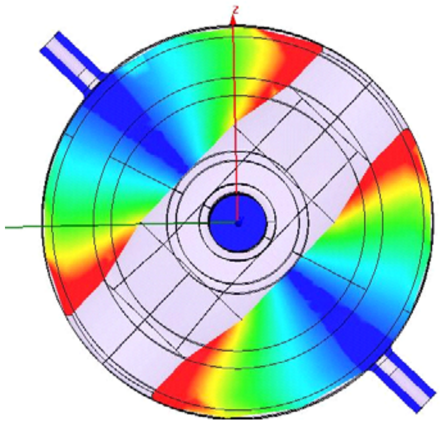

**Figure 10. Normalised integral of squared magnetic field on antenna surface vs. angle of the port with the spoke**

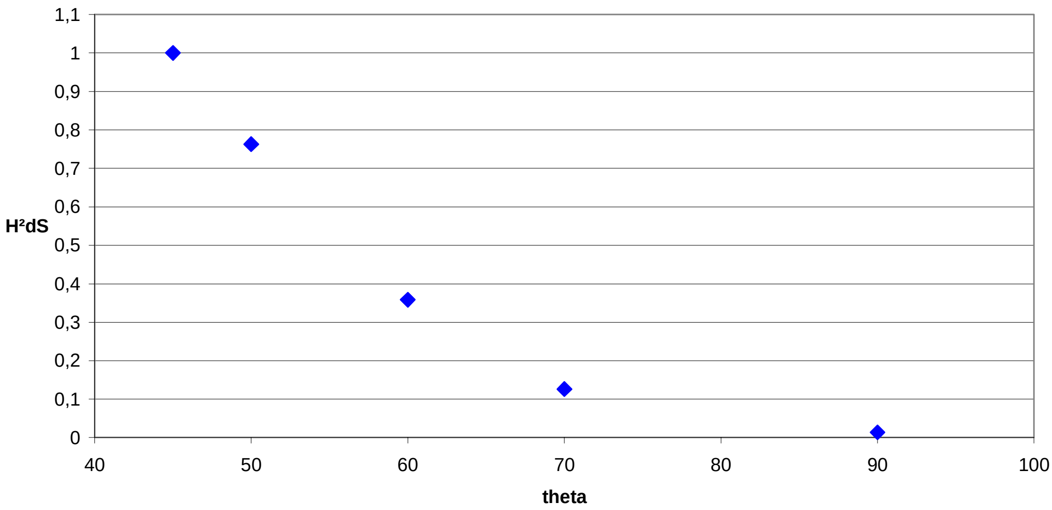


### *Coupling with angle $\theta$ = 90°, antenna position*

The results of the simulations show that the requirements for the coupling factor (regarding the intensity of the beam and the corresponding power to be provided) can be easily reached with the new port position. The position of the antenna is given on the axis of the port. Figures 11and 12 show the simulations results for a $\beta$ = 0.35 cavity and for a $\beta$ = 0.15 cavity.

### Studies in progress on power coupler

In addition to the developments on the spoke cavities, the associated power coupler is also under study. The main work, at this moment, concerns the ceramic window. Many window shapes have already been investigated to choose the accurate one. Table 4 shows the main parameters that will determinate which window to choose for the spoke cavity. From these results it can be inferred that the cylindrical type of window, shown in Figure 13, is the most appropriated for spoke coupler.

**Figure 11. $Q_i$ vs. antenna position (mm)**

*On the left of the vertical line, inside the cavity, on the right, inside coupling port for AMANDA (b = 0.35)*

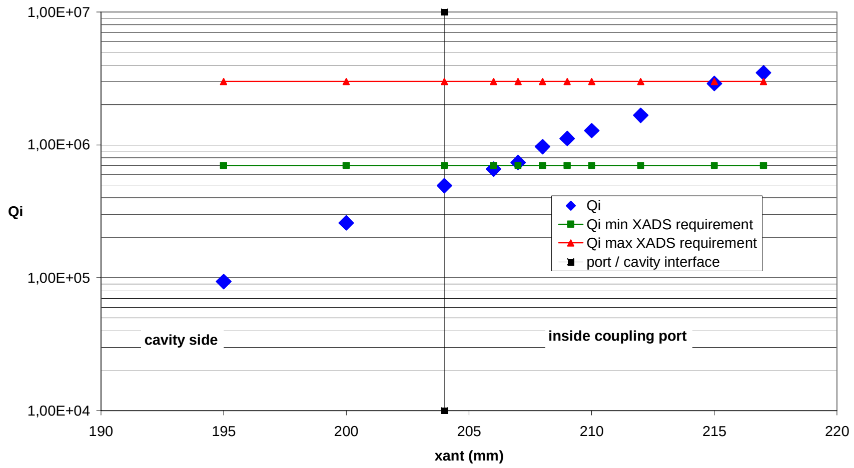


**Figure 12. $Q_i$ vs. antenna position (mm) for b = 0.15 spoke cavity**

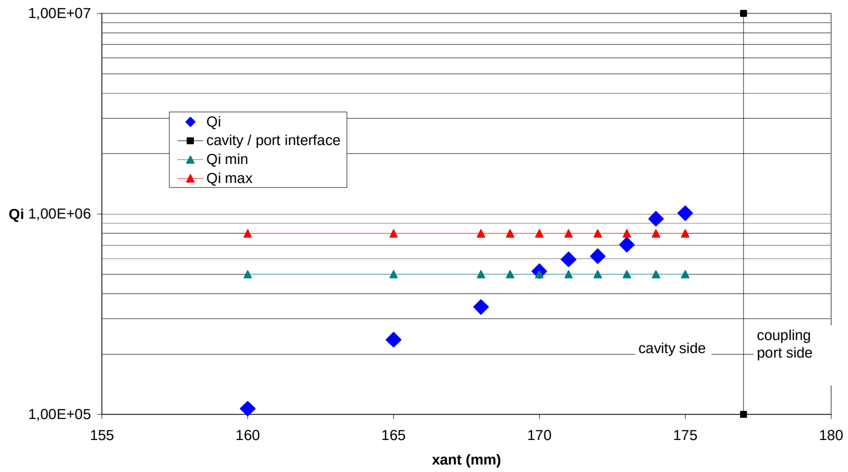


**Table 4. Main parameters of different window shapes for spoke power coupler**

| | Window type | | | | |
|---|---|---|---|---|---|
| | Disc with chokes | Disc (no chokes) | Cylindrical | Waveguide/ coax | Disc with chokes |
| **S11 at 352 MHz (dB)** | -55.4 | -58 | -45.17 | -60 | -40.2 |
| **Bandwidth (MHz)** | >1 000 | 760 | 410 | 6 | 8 |
| **Esurf max (V/m)** | 9.88E+04 | 1.24E+05 | 1.50E+04 | 1.24E+04 | 2.30E+04 |
| **Losses inside the window (W)** | 60 | 71.75 | 68.2 | 147 | 33 |
| **% Pinc** | 0.30% | 0.36% | 0.34% | 0.74% | 0.17% |
| **Window volume (cubic mm)** | 2.86E+04 | 1.65E+04 | 8.11E+04 | 1.61E+06 | 1.37E+05 |
| **Volumic losses ($W/mm^3$)** | 2.10E-03 | 4.34E-03 | 8.41E-04 | 9.14E-05 | 2.41E-04 |

**Figure 13. Cylindrical window simulation model**

*Darker shading (orange) – conductors, lighter shading (green) – ceramic window*

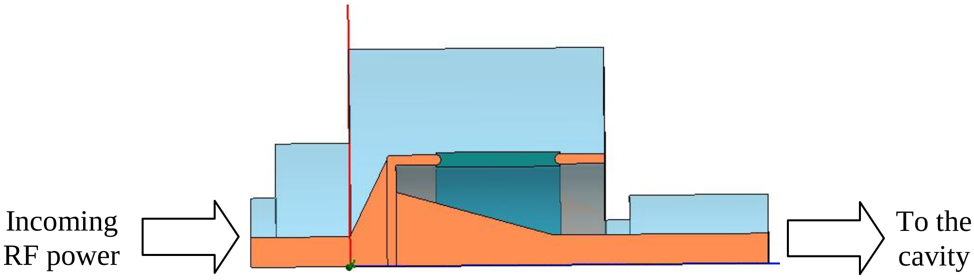


## Conclusion

The overall design achieved concerning AMANDA and its mechanical stability show that this cavity is a very good component for a fault tolerant linac for PDS-XADS. Indeed, the good performances ($E_{acc}$ max = 12.5 MV/m and $Q_0 = 1.5 \cdot 10^9$ at $E_{acc}$ = 7MV/m) are much higher than the established requirements ($E_{acc}$ = 7 MV/m with $Q_0 = 7 \cdot 10^5$) and allow de-rated mode operation that is an *a priori* asset for reliability.

*Acknowledgements*

The author would like to thank Alex C. Mueller and the team working on spoke cavities at IPN Orsay for their help.

## REFERENCES

[1] Pierini, P., “ADS Reliability Activities in Europe”, these proceedings.

[2] Vandeplassche, D., *et al*., “The PDS-XADS Reference Accelerator”, these proceedings.

## TABLE OF CONTENTS

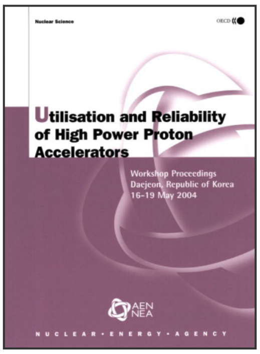


**From:**

# Utilisation and Reliability of High Power Proton Accelerators

## Workshop Proceedings, Daejeon, Republic of Korea, 16-19 May 2004

**Access the complete publication at:**

https://doi.org/10.1787/9789264013810-en

**Please cite this chapter as:**

Miélot, C. (2006), "Spoke Cavities: An Asset for the High Reliability of a Superconducting Accelerator", in OECD/Nuclear Energy Agency, *Utilisation and Reliability of High Power Proton Accelerators: Workshop Proceedings, Daejeon, Republic of Korea, 16-19 May 2004*, OECD Publishing, Paris.

DOI: https://doi.org/10.1787/9789264013810-20-en